

# Bag of Tricks for Long-Tail Visual Recognition of Animal Species in Camera-Trap Images

Fagner Cunha\*, Eulanda M. dos Santos, Juan G. Colonna

*Federal University of Amazonas, Manaus, Amazonas, Brazil*

---

## Abstract

Camera traps are a method for monitoring wildlife and they collect a large number of pictures. The number of images collected of each species usually follows a long-tail distribution, i.e., a few classes have a large number of instances, while a lot of species have just a small percentage. Although in most cases these rare species are the ones of interest to ecologists, they are often neglected when using deep-learning models because these models require a large number of images for the training. In this work, a simple and effective framework called Square-Root Sampling Branch (SSB) is proposed, which combines two classification branches that are trained using square-root sampling and instance sampling to improve long-tail visual recognition, and this is compared to state-of-the-art methods for handling this task: square-root sampling, class-balanced focal loss, and balanced group softmax. To achieve a more general conclusion, the methods for handling long-tail visual recognition were systematically evaluated in four families of computer vision models (ResNet, MobileNetV3, EfficientNetV2, and Swin Transformer) and four camera-trap datasets with different characteristics. Initially, a robust baseline with the most recent training tricks was prepared and, then, the methods for improving long-tail recognition were applied. Our experiments show that square-root sampling was the method that most improved the performance for minority classes by around 15%; however, this was at the cost of reducing the majority classes' accuracy by at least

---

\*Corresponding author

*Email address:* `fagner.cunha@icomp.ufam.edu.br` (Fagner Cunha)

3%. Our proposed framework (SSB) demonstrated itself to be competitive with the other methods and achieved the best or the second-best results for most of the cases for the tail classes; but, unlike the square-root sampling, the loss in the performance of the head classes was minimal, thus achieving the best trade-off among all the evaluated methods. Our experiments also show that Swin Transformer can achieve high performance for rare classes without applying any additional method for handling imbalance, and attains an overall accuracy of 88.76% for the WCS dataset and 94.97% for Snapshot Serengeti using a location-based training/test partition. Despite the improvement in the tail classes' performance, our experiments highlight the need for better methods for handling long-tail visual recognition in camera-trap images, since state-of-the-art approaches achieve poor performance, especially in classes with just a few training instances.

*Keywords:* Long tail, Camera traps, Animal species recognition, Deep learning

---

## 1. Introduction

Wildlife monitoring using camera traps is a well-established, non-invasive, and cost-effective method that has been used for decades to collect data on animals in their daily lives. The collected data can be used to support ecological studies on the terrestrial vertebrate community, such as species occupancy, diversity and abundance, community structure, and animal behavior (Ahumada et al., 2013). These cameras are usually activated by motion sensors or at programmed time intervals to record short sequences of images or videos (He et al., 2016b). They are able to produce a large number of pictures; for instance, the Snapshot Serengeti project captured 3.2 million images between June 2010 and May 2013 over six seasons (Swanson et al., 2015b), with this number growing to 7.1 million images over eleven seasons in recent years (Lila.science, 2022b). However, processing this amount of data to extract information is expensive and time-consuming if done manually by experts or citizen scientists. Using the Snapshot Serengeti project as an example again, its volunteers donated more

than 17,000 hours of effort to manually label the 3.2 million images in the original dataset (Norouzzadeh et al., 2018). Nevertheless, recruiting such a large community of volunteers may be unfeasible for small-scale projects or those studies with a less charismatic fauna.

In the last decade, deep learning has become the dominant approach in image analysis and has been investigated for automatically extracting information from camera-trap data in various tasks, such as filtering empty images (Willi et al., 2019; Cunha et al., 2021; Yang et al., 2021a,b,c), classifying animal species (Villa et al., 2017; Beery et al., 2018; Norouzzadeh et al., 2018; Tabak et al., 2019; Willi et al., 2019; Schneider et al., 2020; Kutugata et al., 2021; Zhu et al., 2022), counting individuals (Norouzzadeh et al., 2018, 2021), and identifying behavior (Norouzzadeh et al., 2018; Schindler & Steinhage, 2021). Meanwhile, several platforms have been developed to assist researchers in extracting information and speeding up this process using deep-learning models. Some of these platforms even allow a wider audience of camera-trap users to train their own models with user-friendly interfaces. For example, MegaDetector (Beery et al., 2019) is a generalist model trained to localize animals, people, and vehicles, helping users to identify animals but not classifying them at the species level, and is effective in filtering empty images. While MegaDetector is based on the language Python, the Machine Learning for Wildlife Image Classification (MLWIC2) package was developed in R to facilitate the use of deep-learning models by biologists, since they are usually more familiar with this language (Tabak et al., 2020). MLWIC2 provides trained models for animal species classification and for filtering empty images, and also allows users to train new models. Other platforms have also developed graphical user interfaces, such as Wildlife Insights (Ahumada et al., 2020), Conservation AI (Chalmers et al., 2019), IFLA (Xi et al., 2021), and Animal Scanner (Yousif et al., 2019), to aid researchers in extracting information.

Unlike traditional machine-learning methods, which are based on hand-crafted features, deep-learning models automatically learn multiple levels of representation directly from the data (Bengio, 2012). To achieve this, deep-learning

models, generally deep neural networks, add more layers and more units within a layer, while also needing large datasets to learn these increasingly complex representations (Goodfellow et al., 2016). Despite the large amount of camera-trap data available, extracting information from these images is difficult because various factors make this task hard even for humans, such as animals too far from the camera, camouflage, animals in a complex pose, and poor illumination, among others, as shown in the literature (Villa et al., 2017; Norouzzadeh et al., 2018). Another major problem with camera-trap data is the extreme imbalance among categories as shown in Figure 1, in which some species have many images while others have just a few, following a long-tail distribution. As reinforced by Schneider et al. (2020), models generally achieve poor recall scores for species with fewer training images, although these rare species are often the ones of greatest interest to ecologists.

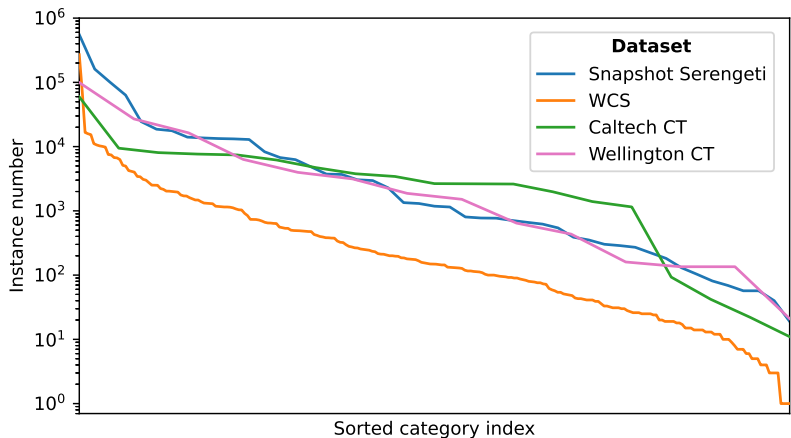


**Fig. 1.** The number of instances per category observed in the camera-trap datasets used in this work follows a long-tail distribution. Categories are sorted by the number of instances in the training set and aligned among datasets for better visualization.

Many works in the literature on machine learning have proposed techniques for addressing the long-tailed issue, such as re-sampling the data (Kang et al., 2020), re-weighting the loss (Cui et al., 2019), or creating multiple branches in

the networks (Li et al., 2020; Zhou et al., 2020; Cai et al., 2021). Despite this, most of the works for classifying animal species in camera-trap images do not apply any method for handling long-tail classification. Some works remove the tail classes (Villa et al., 2017; Willi et al., 2019) or group them into generic categories (Zualkernan et al., 2020). For instance, Villa et al. (2017) evaluate an artificially balanced version of the Snapshot Serengeti dataset, in which the training instance was reduced from 548,608 images to 26,000. However, this approach can reduce the amount of relevant information used to train the model, since diversity and the amount of data available for training are crucial to allow models to generalize well (Chou et al., 2020). Norouzzadeh et al. (2018) apply re-weighting and over-sampling strategies to train a ResNet-152 model for the Snapshot Serengeti dataset. Their results show a 40% improvement for some rare classes but, for other classes, there was a decrease in performance. Schneider et al. (2020) also used over-sampling combined with data augmentation to handle the extreme imbalance in their dataset. Yang et al. (2021a) conducted a systematic study of class imbalance in the Snapshot Serengeti dataset, and evaluated various levels of class imbalance and their impact on model performance. However, this study considered only the problem of filtering empty images. Nevertheless, it is difficult to generalize the results presented in these works since most of the experiments were carried out on a single dataset. Schneider et al. (2020), for example, did not reach a general conclusion, and recommended gathering more images for instance, which is not always feasible.

Based on the empirical observation that square-root sampling (Kang et al., 2020), a type of re-sampling strategy, was the method that most improved the performance of the tail classes, though at the cost of strongly degrading the head classes, in this work a framework called Square-root Sampling Branch (SSB) is proposed, which combines the predictions of two classification branches: one trained using square-root sampling and the other one trained without any additional method for long-tail classification. To achieve more general conclusions, a systematic study of our proposed method was performed, as well as of other state-of-the-art methods for handling long-tail distribution in four camera-trap

datasets – Snapshot Serengeti, WCS, Caltech Camera Traps, and Wellington Camera Traps – and four families of computer vision models: ResNet, EfficientNet, MobileNetV3, and Swin Transformer. A strong baseline training procedure, which included the most recent training innovations, commonly called tricks, was also prepared and was responsible for great improvements of classical architectures such as ResNet.

Another issue is that the high classification accuracy reported in the literature, such as 96.6% achieved by Norouzzadeh et al. (2018) and 98% by Tabak et al. (2019), is usually not achieved when using deep-learning models to classify images from new locations. As shown by various authors (Beery et al., 2018; Tabak et al., 2019; Schneider et al., 2020), it is difficult to reach high accuracy rates even in images from new locations in the same region of the images used to train the models. Due to this fact, to better assess the models, recent works propose to use training/test splitting based on locations (Beery et al., 2018; Schneider et al., 2020). In this case, images used for testing are selected from locations that are different from the training ones. This approach is important in the context of long-tail visual recognition because, if species occurrences are concentrated in a few locations, the model can learn spurious correlations, for example, associating the species to the background, which is usually static for each camera-trap node. Therefore, a location-based split can provide a better assessment of the generalizability of the models. An additional strategy is to use an object detector to localize animals before classifying them, thus appropriately reducing the background influence (Schneider et al., 2018; Beery et al., 2019).

As the contributions of this paper, we can highlight:

- The proposal of a simple and effective framework called Square-root Sampling Branch (SSB) for long-tail visual recognition, which achieves a better trade-off as it improves performance in tail classes at the cost of head classes’ accuracy when compared to the state-of-the-art methods.
- New baselines in camera-trap datasets are established using training/test

partitioning that is based on locations by combining the most recent training tricks with both traditional architectures, such as ResNet-50, and newer ones such as Swin Transformer.

- Our experiments show that Swin Transformer can achieve excellent results in camera-trap datasets even without using any additional method for handling the long-tail issue.

To aid readers who may not be familiar with certain terms related to computer science, a glossary of terms have been included in the Supplementary Materials (see Appendix A).

## 2. Materials and Methods

In long-tail recognition problems, the classes in the datasets used to train the models follow a long-tail distribution, as occurs with camera-trap datasets. Our methodology was built to assess the effectiveness of our proposed SSB framework in improving the recognition performance in the tail classes and comparing it with methods available in the literature. First, a strong baseline was trained with several recent training tricks available in the literature. Then, each long-tail method was applied and evaluated using appropriate metrics to assess long-tail performance. To reach a more general conclusion, the performance of the methods on four long-tail camera-trap datasets with different characteristics and four families of computer vision models were evaluated.

In the next section, the datasets, the chosen computer vision architectures, and the baseline training procedure are described. Then, the families of methods for long-tail recognition and the selected methods used in this work are presented. Following this, a description of our proposed Square Root Sampling Branch (SSB) framework is given and, finally, the metrics used to evaluate the models are described.

### 2.1. Datasets

This section describes the four camera-trap datasets used in this study: Snapshot Serengeti, Caltech Camera Traps, WCS Camera Traps, and Wellington Camera Traps. These datasets were obtained from different regions around the globe and have different characteristics, such as the number of training instances, imbalance factor, and available species. While annotations for these datasets are provided for bursts (i.e., a sequence of images), we assign each image the label inherited from its burst annotations during the training process. However, this approach may result in mislabeling, especially when the animal appears in only a few images within a burst. Since manual verification was not feasible due to the large amount of images in the datasets, the data was used as provided, as has been done in prior studies (Villa et al., 2017; Norouzzadeh et al., 2018). Nonetheless, it is important to note that the recommended approach is to have annotations at an image-level, as this provides more accurate training data. Following the recent recommendations, the datasets were split into training/validation/test partitions based on camera locations to better assess the models’ generalization. Additionally, images were removed from all classes which, due to the location-based split, do not have instances in the training or test partitions. Images containing more than one species and also corrupted pictures were also removed. Table 1 summarizes the number of images used from each dataset in this work. All of these datasets follow a long-tail distribution, as shown in Figure 1, in which a few classes (head) concentrate most of the instances and the remaining classes have just a few samples in comparison.

***Snapshot Serengeti*** (Swanson et al., 2015a). This dataset is composed of more than 7 million images obtained from 225 locations spread across the Serengeti National Park in Tanzania, and is divided into 11 seasons. To maintain consistency with the literature, only the first six seasons are used in this work. The recommended training/validation partitions based on locations were used (Lila.science, 2022b), with the validation set being used to evaluate the models. To adjust the hyperparameters, a mini-validation (minival) partition was held



**Table 1**

Number of images and locations per partition used from each dataset.

Dataset	Classes	Training		Validation		Test	
		# loc	# instances	# loc	# instances	# loc	# instances
Snapshot Serengeti	47	156	1,059,793	23*	360,317	46*	738,404
Caltech CT	19	80	122,693	20*	57,162	40*	61,665
WCS	247	2,506	599,040	313	79,906	314	62,734
Wellington CT	14	111	160,937	36	49,127	35	55,424

\* As long as there are no official test sets for Snapshot Serengeti and Caltech CT datasets, their recommended validation sets were used as the test sets in this work. For these datasets, validation sets (which were called minival) were held out from their respective training sets following the locations selected by Cunha et al. (2021).

out from the training set using the locations selected by Cunha et al. (2021). Specifically for this dataset, given that images from empty bursts (background or blank) are near identical, only one picture was picked at random from each empty burst. This also helps to keep a tractable number of images to train the models. In total, approximately 2 million pictures distributed in 47 categories were used.

**Caltech Camera Traps** (Beery et al., 2018). This dataset is composed of approximately of 240,000 images from 140 locations in the southwestern United States. The recommended location-based training/validation partitions were used (Lila.science, 2022a), and, as for the Snapshot Serengeti, the validation set was used for testing, and a mini-validation partition was created from the training set for hyperparameter adjustment based on locations selected by Cunha et al. (2021).

**WCS Camera Traps** (Lila.science, 2022c). This dataset is provided by the Wildlife Conservation Society, and it is composed of 1.4 million images of around 675 species from 12 countries, thus making it one of the most diverse datasets publicly available. In our experiments, the recommended training/validation/test partitions based on locations were used. However, since some locations were not allocated to any partition, images from them were not used. The generic unknown categories and those not related to animals, such

as misfire, start, and end were also manually removed. As images from classes without instances in training or testing sets were also removed, the resulting selected subset is composed of images from 247 categories.

**Wellington Camera Traps** (Anton et al., 2018). This dataset is originally composed of around 270,000 images collected from 187 camera locations in the Wellington region of New Zealand. The training/validation/test proposed by Shashidhara et al. (2020) was used. Images marked as unclassifiable were removed, in addition to images from the categories not present in the training or test partition, thus resulting in a dataset of around 265,000 images from 14 categories. Unlike the other datasets, whose empty class is the majority category, in this dataset the generic bird category has three times more images than the empty category, and has the second-largest number of instances.

## 2.2. Architectures

Four popular computer vision architectures with different purposes and characteristics were chosen to assess whether long-tail classification methods work well on different backbones: ResNet-50 (He et al., 2016a), MobileNetV3-Large (Howard et al., 2019), EfficientNetV2-B2 (Tan & Le, 2021), and Swin-S (Liu et al., 2021). First, ResNet-50 was selected because it is the most common baseline for almost any method in computer vision. As using computer vision models directly on edge devices for processing camera-trap data has gained attention in the literature (Elias et al., 2017; Zualkernan et al., 2020; Cunha et al., 2021; Zualkernan et al., 2022), MobileNetV3-Large was chosen as a benchmark for this situation. For the state-of-the-art families of EfficientNet (Tan & Le, 2019) and Swin Transformer (Liu et al., 2021) models, lightweight versions – EfficientNetV2-B2 and Swin-S, respectively – were chosen, since most of the camera-trap practitioners usually do not have access to powerful computers to run big models (Schneider et al., 2020). Table 2 shows the number of model weights (without the classification layer, which varies according to the dataset), input size, and number of FLOPs for each of these models. FLOPs refers to the

number of floating-point operations (multiply-adds) performed by a model, and is commonly used as a measure to estimate the theoretical computational complexity (Zhang et al., 2018). These details can be used to compare architectures in terms of hardware requirements.

**Table 2**

Details of the architectures used. The number of FLOPs (in billions) is calculated from the literature considering the ImageNet classification head (1,000 classes).

Architecture	# weights	input size	FLOPs
ResNet-50	23,587,712	224 x 224	4.1B
MobileNetV3-Large	4,226,432	224 x 224	0.22B
EfficientNetV2-B2	8,769,374	260 x 260	1.7B
Swin-S	49,173,398	224 x 224	8.7B

### 2.3. Baseline training settings

As shown recently (He et al., 2019; Bello et al., 2021; Wightman et al., 2021), improved training strategies are responsible for significant gains in the accuracy of classical architectures such as ResNet-50. Following these ideas, several tricks were included in our baseline training procedure, and these are described below.

**Image preprocessing.** Initially, all images were resized so that the largest dimension was at most 768 px, and the smallest one was at least 450 px. During training, first, a rectangular region of aspect ratio sampled in  $[3/4, 4/3]$  and area in  $[65\%, 100\%]$  was randomly cropped and resized to the input size of the architecture. Next, the image was flipped horizontally with a 50% probability. Then, RandAugment (Cubuk et al., 2020) was used, which is a method that applies a random sequence of image distortions, such as rotation, contrast, and brightness distortions, to dynamically augment the data during the training. This method has two hyperparameters:  $N$ , which is the number of distortions applied sequentially, and  $M$ , which is the magnitude of all distortions. In this work, we set  $N = 2$  and  $M = 9$  as parameters for RandAugment. Finally, the

image was rescaled to match the input scale of each architecture, as shown in Table 3. During the evaluation, the preprocessing consists only of resizing the image to the input architecture size and rescaling.

**Table 3**

Input scaling procedure for each architecture.

Architecture	Scaling Procedure
ResNet-50	Convert from RGB to BGR, zero-center w.r.t. the ImageNet dataset, without scaling
MobileNetV3-Large	Pixels between 0 and 255 (model includes pre-processing layer)
EfficientNetV2-B2	Scale pixels between -1 and 1
Swin-S	Scale pixels between 0 and 1, normalize w.r.t. the ImageNet dataset

**Training procedure.** The models were initialized with ImageNet pre-trained weights, replacing the classifier layer, and, then, were trained with a batch size of 64 for 30 epochs when fine-tuning the whole model or for 12 epochs when training only the classifier layer. The AdamW optimizer (Loshchilov & Hutter, 2019) was employed for training with an initial learning rate of  $10^{-5}$  and weight decay of  $10^{-7}$ . The learning rate was linearly warmed up from 0 to the initial value for two epochs when fine-tuning – one epoch when training only the classifier –, and then decayed to 0 using the cosine schedule (He et al., 2019).

#### 2.4. Training tricks for long-tail visual recognition

This section describes some effective methods for long-tail visual recognition that were evaluated in this work for camera-trap image classification. The methods were grouped into four main families according to their focus: re-sampling the data, re-weighting the loss, using two stages to focus on representation

learning, and creating multiple branches in the network. The method of using an object detector to crop regions of interest from camera-trap images before classifying them was also included in this section. Despite not dealing directly with the imbalance problem, it has been shown in the literature (Schneider et al., 2018; Beery et al., 2019) that this trick improves the recognition score in camera-trap images. Figure 2 illustrates a functional summary of the model training process, highlighting the stages where each method studied in this work operates.

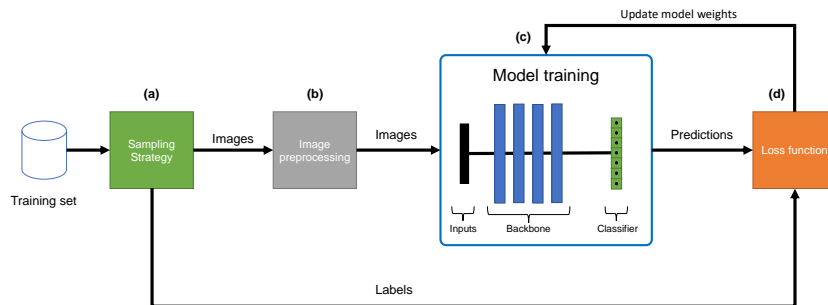


**Fig. 2.** Schematic diagram of model training process. Each method studied in this work operates at one or more stages: re-sampling methods change the sampling strategy (a), re-weighting methods modify the loss function (d), methods using multi-branch networks modify the model structure (c), and two-stage training methods operate by selecting which model weights (c) are trained at each stage. Our proposed SSB method operates by changing both the sampling strategy (a) and the model structure (c). Additionally, cropping images before classification is performed at the image preprocessing stage (b).

#### 2.4.1. Re-sampling

Re-sampling methods attempt to sample the dataset in order to obtain a more balanced data distribution by over- or under-sampling instances according to the number of instances per class. On the one hand, random over-sampling consists of replicating instances from the minority classes; however, this method can lead to overfitting these instances (Chou et al., 2020; Cai et al., 2021). On

the other hand, random under-sampling discards instances from the majority classes, which can degrade the representation learning, especially for extremely imbalanced datasets (Chou et al., 2020).

In some re-sampling strategies, the probability  $p_j$  of sampling an instance from class  $j$  is given by:

$$p_j = \frac{n_j^q}{\sum_{i=1}^C n_i^q}, \quad (1)$$

where  $C$  is the number of training classes,  $n_i$  is the number of training instances from class  $i$ , and  $q \in [0, 1]$ . When  $q = 1$ , each class has a probability  $p_j$  directly proportional to its number of instances, i.e., each instance has the same probability of being sampled, for this reason, this method is known as instance-balanced sampling, and, in practice, it uses the original data distribution (Kang et al., 2020). When  $q = 0$ , each class has an equal probability ( $p_j = 1/C$ ) of being selected, this is also called class-balanced sampling (Kang et al., 2020; Zhang et al., 2021). In this work, following recent literature (Kang et al., 2020; Zhang et al., 2021), an alternative between those two extremes was chosen by setting  $q = 1/2$  – called square-root sampling, since this approach returns a less imbalanced dataset.

#### 2.4.2. Re-weighting

The re-weighting methods work by modifying the loss function in order to re-define the importance given to each class or instance during the training. These methods guide the network on where to pay more attention by assigning different weights to different categories or instances (Kang et al., 2020; Zhang et al., 2021; Wang et al., 2021). One naïve approach is to weight the dataset based on the inverse class frequency or the inverse square root of class frequency (Chou et al., 2020). More sophisticated approaches, such as the Focal loss and the Class-Balanced loss, have been developed and take into consideration factors such as how easy one sample is, or the effective number of samples.

Focal loss (Lin et al., 2017) was proposed in the context of the object detection problem, in which there is an extreme foreground-background class im-

balance. This loss automatically down-weights well-classified samples to make the training focus on hard training instances. To achieve this objective, given a class probability prediction  $p_i$  for the instance  $x_i$ , Focal loss  $L_{focal}$  is defined as

$$L_{focal} = -(1 - p_i)^\gamma \log(p_i), \quad (2)$$

where  $\gamma \geq 0$  is a parameter that controls the rate at which easy examples are down-weighted.

The Class-Balanced loss (CB loss) (Cui et al., 2019) weights each class based on the effective number of samples  $E_n$ , which is given by:

$$E_n = \frac{1 - \beta^n}{1 - \beta}, \quad (3)$$

where  $n$  is the number of samples and  $\beta \in [0, 1)$  is a hyperparameter. Given a class  $j$  with  $n_j$  training samples, the loss  $L$  with respect to this class is weighted by a factor using the effective number of samples:

$$CB(\mathbf{p}, j) = \frac{1}{E_{n_j}} L(\mathbf{p}, j) = \frac{1 - \beta}{1 - \beta^{n_j}} L(\mathbf{p}, j), \quad (4)$$

where  $\mathbf{p}$  denotes the class probabilities estimated by the model.

For representing the re-weighting methods in our experiments, the Class-Balanced Focal (CB-Focal) loss was used, which is the combined version of Focal loss and Class-Balanced loss. In this case,  $L(\mathbf{p}, j)$  in Equation 4 is replaced by  $L_{focal}$  from Equation 2. This loss weights the importance of each instance on the loss from the perspective of both class distribution and sample easiness. In our experiments,  $\beta$  was set to 0.9 and  $\gamma$  to 2.0.

### 2.4.3. Two-stage training

The extensive experiments conducted by Kang et al. (2020) on common long-tail benchmarks showed that data imbalance is not an issue for learning high-quality representations. Their results evidenced that it is possible to attain a good long-tail recognition score by training only the classifier on top of those learned representations. Taking this into account, Kang et al. (2020) propose a two-stage training method for long-tail recognition. In the first stage, the model

is trained using the original unbalanced training distribution. In the second, only the classifier is trained using a balancing method, such as re-weighting or re-sampling.

#### 2.4.4. Multi-branch networks

Methods using multi-branch networks handle the long-tail problem by creating expert branches to treat relatively balanced sub-groups of classes separately. The Bilateral-Branch Network (BNN) (Zhou et al., 2020) uses two backbone branches, one is trained with a uniform sampler and the second one uses a sampler with a reversed distribution w.r.t. the original long-tail distribution; a cumulative learning strategy is then used to combine their output feature vectors. Ally Complementary Experts (ACE) (Cai et al., 2021) works by using multiple expert branches on top of a shared backbone, in which each expert has individual learning blocks and a prediction layer for a diverse but overlapping set of categories. Then, the experts’ predictions are aggregated by averaging the logits that are re-scaled according to the data splits. The main idea is that the dominating categories (head classes) for each expert are different, and the overlapping categories support each other during the aggregation, especially for categories with few samples. Balanced Group Softmax (BAGS) (Li et al., 2020) also uses a shared backbone for representation learning, but the categories are divided into disjoint groups according to the number of instances. It was decided to test the effectiveness of BAGS because the winning team (Cunha, 2021) of the iWildCam 2021 (Beery et al., 2021) – an annual competition on extracting information from camera-trap images – used it.

BAGS is trained in a two-stage fashion. First, the model is trained using a single softmax classification head containing all categories. Then, the classification head is replaced by the new groups of classification heads randomly initialized. Finally, only these heads are trained, with all other weights frozen. Each category  $j$  is assigned to a single group  $G_k$  based on its number of training instances  $n_j$  if  $s_k^l \leq n_j < s_k^h$ , with  $k > 0$ , where  $s_k^l$  and  $s_k^h$  are the minimum and maximum number of instances for the group  $G_k$  and  $s_{k+1}^l = s_k^h$ . In our experi-



ments using BAGS, following the originally proposed method (Li et al., 2020), the categories were split into four groups, with  $s^l$  and  $s^h$  set to  $(0, 10)$ ,  $(10, 10^2)$ ,  $(10^2, 10^3)$ , and  $(10^3, +\infty)$ , and the special group  $G_0$  for foreground/background classification. Each group includes an extra category *others* for the samples from classes belonging to the other groups. To balance training, the *others* category within each batch was undersampled by a factor of  $\beta \times n_k$ , where  $n_k$  is the number of instances from categories belonging to the group in that batch ( $\beta = 8$  was used). During the inference, a softmax is applied to each group and the probabilities are remapped back to the original category order and rescaled by the foreground probability. By this design, classes with a significantly different number of instances are isolated from each other during the training, thus avoiding the tail classes being substantially suppressed by the head classes.

#### 2.4.5. Cropping before classification

As shown in (Schneider et al., 2018) and (Beery et al., 2019), using an object detector to crop regions of interest from camera-trap images before classifying may improve the recognition score. This training trick was included in our experiments to evaluate how it can enhance the species classification when combined with other methods used to tackle the long-tail issue. MegaDetectorV4 (Beery et al., 2019) was used to generate bounding box predictions, which is a general-purpose animal detector based on the object detector Faster R-CNN (Ren et al., 2015) and is trained on a large number of camera-trap images. In our experiments with cropping before classification, MegaDetectorV4 was run on the resized images before the random crop operation in the preprocessing pipeline. Only bounding boxes with a confidence score higher than 0.6 were considered, otherwise, the whole image was used. Then, a squared crop was applied around the bounding box with the highest confidence score. Following this, the preprocessing procedure occurs as described in the baseline training settings (subsection 2.3).

### 2.5. SSB: Square-root Sampling Branch

Our proposed framework is a multi-branch network approach that was inspired by an empirical observation in our preliminary experiments: the square-root sampling strategy was the method that most improved the accuracy of the tail classes over the baseline; however, at the cost of significantly decreasing the performance of the head classes. The question to answer is: is it possible to combine the **S**quare-root **S**ampling **B**ranch (SSB) predictions with the baseline to improve the tail classes with minimal performance degradation for the head classes?

As illustrated in Figure 3, the proposed framework is trained in a two-stage fashion. First, the classifier ( $f_i$ ) and the backbone are trained jointly using the original data distribution (instance-based sampling). For the second stage, the network backbone is frozen and the classifier is replaced by a new randomly initialized one. Then, this new classifier ( $f_{sqr}$ ) is trained using data sampled by the square-root sampling strategy. Both classifiers are connected on top of the backbone during the inference. Their predictions are aggregated by masking the softmax outputs to keep only the head classes probabilities from the  $f_i$  head and the remaining classes probabilities from the  $f_{sqr}$  head.

The  $C$  classes were divided into four groups based on the number of training instances, in which a class  $j$  with  $n_j$  instances belongs to group  $G_k$  if  $s_k^l \leq n_j < s_k^h$ . The limits of each group are set to  $(0, 10)$ ,  $(10, 10^2)$ ,  $(10^2, 10^3)$ , and  $(10^3, +\infty)$ . However, SSB does not have a special group for the background class, with this class belonging to the group  $G_4$ . Given a feature vector  $h$  generated by the backbone and the predictions  $p_i = f_i(h)$  and  $p_{sqr} = f_{sqr}(h)$  generated by each classification head with softmax, the final remapped prediction vector  $p_r$  is given by:

$$p_r = f_r(p_i, p_{sqr}) = Qp_i + (\mathbf{1} - Q)p_{sqr}, \quad (5)$$

where  $Q$  is a matrix  $C \times C$  that masks the softmax outputs based on which

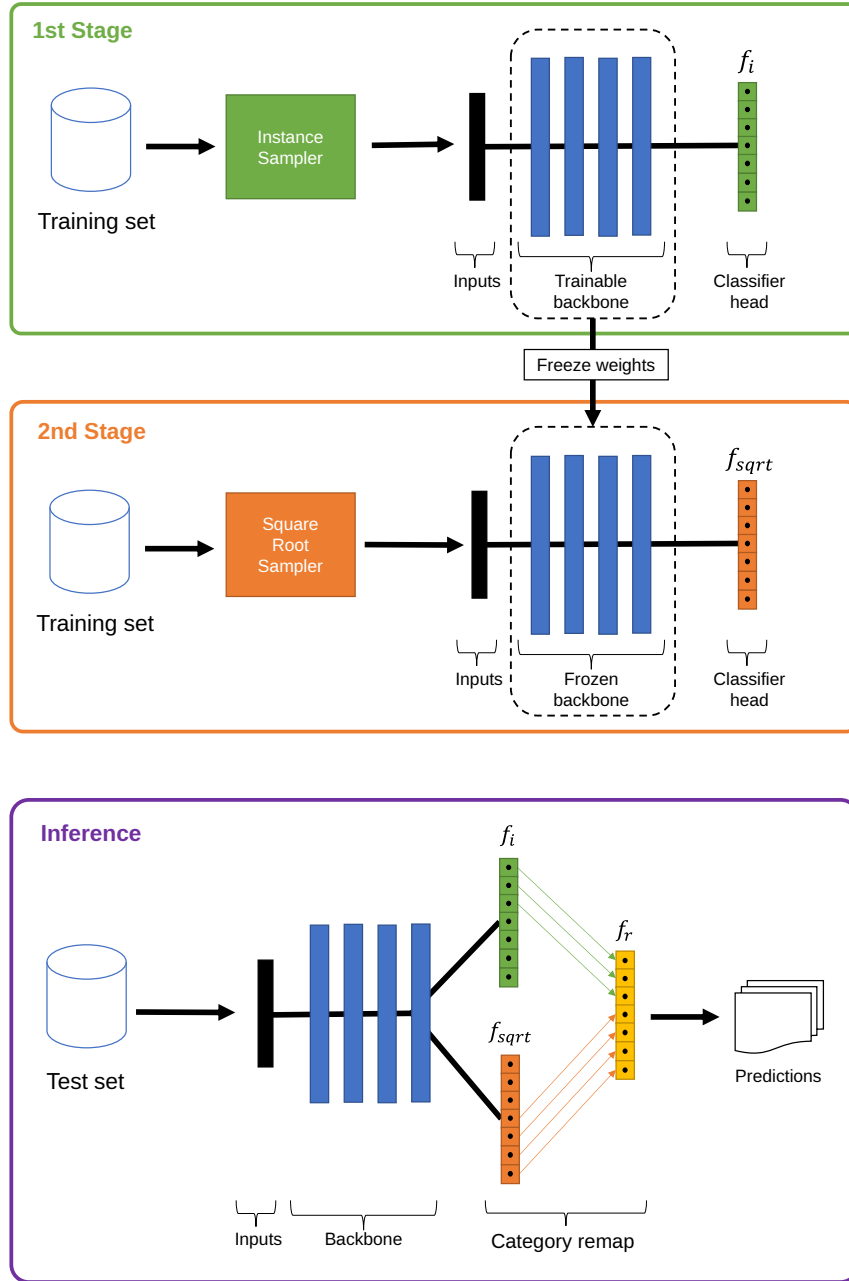


**Fig. 3.** Framework of our Square-root Sampling Branch (SSB). It is trained in two stages. In the first stage, the classifier ( $f_i$ ) and the backbone are jointly trained using the original data distribution. In the second stage, a new classifier ( $f_{sqr}$ ) is trained using square-root sampling and the backbone trained in the first stage is kept frozen. During the inference, predictions from both classifier heads are aggregated by masking the classes to keep the head classes probabilities of  $f_i$  and the remaining classes probabilities of  $f_{sqr}$ .

group a class belongs to:

$$Q = \left\{ q_{a,b} | q_{a,b} = \begin{cases} 1 & \text{if } a = b \text{ and the class } a \in G_4, \\ 0 & \text{otherwise.} \end{cases} \right\}. \quad (6)$$

As with BAGS post-processing, the final prediction vector produced by SSB is not a real probability vector because its sum is not equal to 1.

### 2.6. Evaluation metrics

Traditionally, deep-learning benchmarks use top-1 and top-5 accuracies to evaluate model performance (Russakovsky et al., 2015). However, these metrics are biased towards majority classes for unbalanced datasets, and do not accurately assess the tail classes. Therefore, following Li et al. (2020), the categories in the test set of each dataset were grouped into four bins according to the amount of training instances, and report the accuracy of each bin.  $Bin_i$  contains the categories composed of  $10^{i-1}$  to  $10^i$  instances. Hence,  $Bin_1$  and  $Bin_2$  represent the tail classes, while the  $Bin_3$  and  $Bin_4$  represent the head classes.

In addition to the accuracy using bins, the macro-averaged F1-score is also reported, which is, according to Picek et al. (2022), more suitable for long-tail distributions observed in nature. The F1-score  $F_{1_i}$  of a class  $i$  is the harmonic mean of its precision  $p_i = \frac{tp_i}{tp_i + fp_i}$  and recall  $r_i = \frac{tp_i}{tp_i + fn_i}$ . True positive ( $tp_i$ ) is the number of correct predictions for class  $i$ , False positive ( $fp_i$ ) is the number of instances incorrectly classified as belonging to  $i$ , and False negative ( $fn_i$ ) is the number of instances from class  $i$  wrongly classified as not belonging to  $i$ . The macro-averaged F1-score  $F_1^m$  across  $C$  classes is the mean of the class-wise F1-score:

$$F_1^m = \frac{1}{C} \sum_{i=1}^C F_{1_i} = \frac{1}{C} \sum_{i=1}^C \left( 2 \times \frac{p_i \times r_i}{p_i + r_i} \right). \quad (7)$$

## 3. Experiments and Results

Our experiments were broken down into three main series. In the first, our proposed method SSB is compared to three two-stage methods for long-tail

problems, as well as the baseline. In the second series, the same methods are compared, but using cropped images as inputs instead of the entire images. Finally, in the third series, SSB is compared to single-stage training methods. The results presented in this section were obtained using the test sets specified for each dataset in Table 1.

### 3.1. Comparison between SSB and two-stage methods for long-tail visual recognition

In the first experiment, the effectiveness of our proposed SSB method when using the full image as input for the training and testing stages was evaluated. As our proposed method is trained using a two-stage strategy, in this experiment, only the results with two-stage training methods were compared. Initially, each architecture was trained using our baseline training settings, and then each long-tail method was applied to the classifier layer, though keeping the backbone frozen during the second-stage training. This allows a fair comparison between the methods in terms of the representation learned by the backbone.

The accuracy results are shown in Table 4. The proposed SSB consistently improved accuracy for  $Bin_1$ ,  $Bin_2$ , and  $Bin_3$  when compared to the baseline for almost all cases, with a minimal loss in the head class accuracy ( $Bin_4$ ), and achieved the best or the second-best accuracy per bin for most of the cases. The best results for  $Bin_1$ ,  $Bin_2$ , and  $Bin_3$  were achieved by the square-root sampling, with an improvement ranging from 3% to more than 15% over the baseline. However, such an improvement came at the cost of reducing the accuracy of the majority classes ( $Bin_4$ ) by at least 3%. This aspect may be observed in the overall accuracy, since the square-root sampling achieved the worst results among all the methods. On the other hand, BAGS achieved the best overall accuracy results for some cases; while, in others, it even reduced the accuracy for the tail classes compared to the baseline. All methods, however, failed to improve the performance on tail classes ( $Bin_2$ ) for the smaller datasets (Caltech and Wellington). In this case, accuracies were close to zero.

In terms of the macro-averaged F1-score, SSB achieved a score that was

higher than the other methods for most datasets and architectures, as shown in Figure 4. For all the datasets, the Swin-S trained with the baseline settings attained the best macro F1-score among all architectures, with Swin-S trained with SSB having the second-best result. Figure 5a shows the increment/decrement of the F1-score class-wise over the baseline for ResNet-50 in the WCS dataset after applying each long-tail method. SSB is the method with the most consistent increment in terms of F1-score across classes for ResNet-50. Figure 5b shows that the decrease in F1-score for the Swin-S is generalized over all classes, with SSB being the method that lowers the F1-score the least.

### 3.2. Comparison between methods when using cropped images

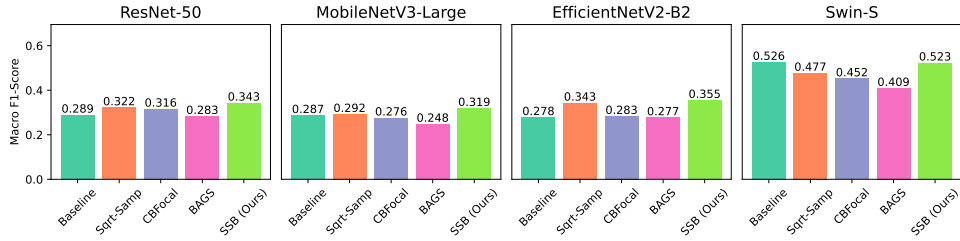
In this experiment, an assessment was made to see whether using an object detector before classifying an animal can improve the recognition score for the tail classes. The same settings from the previous experiment were used, except for using MegaDetectorV4 to generate cropped regions around animals as inputs, though reverting back to the whole image when the confidence score was less than 0.6. For the pre-cropping experiments, the Snapshot Serengeti dataset was not used due to the time required to generate bounding boxes with MegaDetectorV4 and run the experiments with the large quantity of images available.

As shown in Table 5, there was a general accuracy and macro F1-score increase when the models were trained using cropped images. However, these results follow the same pattern observed when using the entire image as the input. Specifically, square-root sampling attained the highest improvements for the tail classes at the cost of reducing performance for the head classes. Our proposed SSB was able to improve the tail classes’ accuracy with minimal accuracy loss for the head classes. In addition, it attained the best macro F1-score in most of the cases. Lastly, Figure 6 shows some sample predictions for pictures randomly picked from the WCS dataset with bounding boxes generated by MegaDetectorV4.

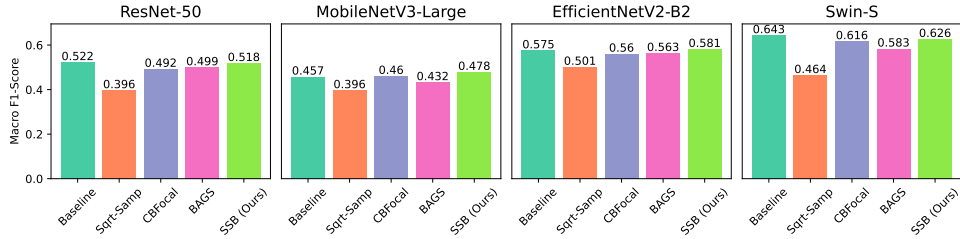
**Table 4**

Comparison between SSB accuracy with different methods for long-tail classification of different models and datasets when using the entire image as the input. Bold and underlined values, respectively, indicate the best and second-best result for each model and dataset combination.  $Acc_i$  is the top-1 accuracy for the  $Bin_i$ . As some category bins do not occur in some of the datasets, in this case, the corresponding column was removed.

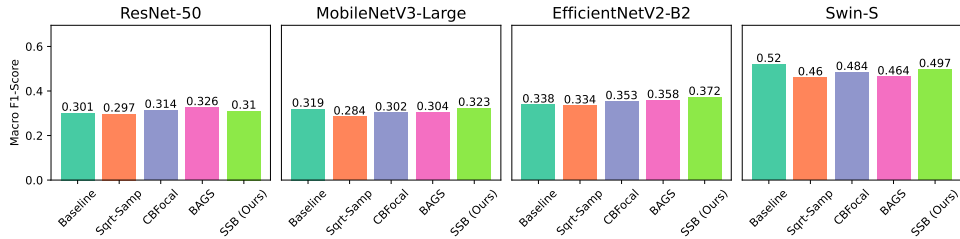
Model	Training	WCS					Snapshot Serengeti				Caltech CT			Wellington CT			
		$Acc_1$	$Acc_2$	$Acc_3$	$Acc_4$	$Acc_{all}$	$Acc_2$	$Acc_3$	$Acc_4$	$Acc_{all}$	$Acc_2$	$Acc_4$	$Acc_{all}$	$Acc_2$	$Acc_3$	$Acc_4$	$Acc_{all}$
ResNet-50	Baseline	0.00	13.05	32.06	<b>85.02</b>	<u>81.53</u>	2.90	44.82	<u>92.96</u>	<u>92.79</u>	0.00	44.95	42.19	0.0	4.58	<b>75.66</b>	72.23
	Sqrt-Samp	<b>16.25</b>	<b>28.94</b>	<b>48.98</b>	75.38	73.47	<u>6.52</u>	<b>51.58</b>	87.29	87.16	0.00	39.59	37.16	0.0	<u>10.65</u>	70.91	68.01
	CBFocal	5.00	14.42	40.61	83.41	80.43	0.72	38.66	92.88	92.69	0.00	44.47	41.74	0.0	4.84	75.12	71.73
	BAGS	<b>16.25</b>	14.19	34.84	84.43	81.14	<b>9.42</b>	41.27	<b>93.12</b>	<b>92.94</b>	<b>1.56</b>	<b>48.04</b>	<b>45.19</b>	0.0	<b>25.92</b>	75.00	<b>72.64</b>
	SSB (Ours)	<u>15.00</u>	<u>21.79</u>	<u>40.97</u>	<u>84.85</u>	<b>81.91</b>	5.07	<u>48.16</u>	92.91	92.75	<u>0.03</u>	<u>46.09</u>	<u>43.26</u>	0.0	5.51	<u>75.62</u>	<u>72.24</u>
MBNetV3	Baseline	0.00	11.92	36.52	<b>84.24</b>	<u>80.98</u>	2.17	29.78	<b>92.73</b>	<u>92.52</u>	0.00	<b>46.14</b>	<b>43.31</b>	0.0	5.70	<b>75.65</b>	<u>72.28</u>
	Sqrt-Samp	<u>7.50</u>	<b>28.26</b>	<b>46.85</b>	76.71	74.61	<u>4.35</u>	<b>43.95</b>	87.62	87.47	<b>0.16</b>	37.76	35.45	0.0	<u>21.68</u>	70.45	68.10
	CBFocal	0.00	9.19	36.98	79.41	76.42	0.72	29.78	92.44	92.23	0.00	41.27	38.74	0.0	4.58	74.94	71.55
	BAGS	<b>10.00</b>	10.44	28.68	<u>84.09</u>	80.48	<b>5.07</b>	28.78	92.19	91.97	0.00	43.96	41.26	0.0	<b>23.41</b>	74.02	71.58
	SSB (Ours)	1.25	<u>20.32</u>	<u>40.43</u>	83.99	<b>81.04</b>	3.62	<u>36.97</u>	<u>92.72</u>	<b>92.53</b>	<u>0.11</u>	<u>45.93</u>	<u>43.12</u>	0.0	13.54	<u>75.34</u>	<b>72.36</b>
EffV2-B2	Baseline	0.00	10.22	32.31	86.35	82.75	2.90	53.71	93.82	93.68	<u>0.08</u>	56.36	52.91	0.0	5.70	<u>77.11</u>	73.67
	Sqrt-Samp	<b>10.00</b>	<b>22.36</b>	<b>50.34</b>	78.24	76.12	<u>6.52</u>	<b>59.25</b>	90.46	90.35	0.00	51.15	48.01	0.0	<u>8.06</u>	74.14	70.95
	CBFocal	0.00	4.20	35.55	<b>87.20</b>	<b>83.62</b>	0.00	46.51	<u>94.51</u>	<u>94.34</u>	0.00	57.36	53.83	0.0	4.09	<b>77.31</b>	<u>73.78</u>
	BAGS	1.25	7.15	32.99	<u>87.01</u>	<u>83.37</u>	<b>7.25</b>	51.45	<b>94.77</b>	<b>94.62</b>	<b>0.26</b>	<u>58.88</u>	<u>55.28</u>	0.0	<b>30.05</b>	76.00	<b>73.79</b>
	SSB (Ours)	<u>7.50</u>	<u>18.39</u>	<u>42.39</u>	86.18	83.17	5.80	<u>55.96</u>	93.81	93.67	<u>0.08</u>	<b>59.82</b>	<b>56.15</b>	0.0	6.75	77.01	73.62
Swin-S	Baseline	<u>8.75</u>	37.12	62.99	<b>90.86</b>	<b>88.76</b>	10.87	60.42	<b>95.09</b>	<b>94.97</b>	<b>4.17</b>	<u>68.94</u>	<u>64.96</u>	0.0	7.61	<b>78.94</b>	<u>75.51</u>
	Sqrt-Samp	<b>16.25</b>	<b>44.84</b>	<b>67.22</b>	83.49	82.13	13.04	<b>64.85</b>	89.08	88.99	1.08	64.95	61.02	0.0	<u>13.09</u>	76.54	73.48
	CBFocal	0.00	25.09	56.57	90.32	87.78	4.35	53.71	94.97	94.82	<u>3.78</u>	<b>69.61</b>	<b>65.57</b>	0.0	5.44	78.49	74.98
	BAGS	6.25	21.68	52.33	90.08	87.32	<b>15.22</b>	52.32	94.81	94.67	3.67	66.01	62.18	0.0	<b>19.65</b>	78.62	<b>75.78</b>
	SSB (Ours)	<b>16.25</b>	<u>40.18</u>	<u>64.91</u>	<u>90.65</u>	<u>88.69</u>	<u>11.59</u>	<u>61.94</u>	<u>95.05</u>	<u>94.93</u>	1.08	67.57	63.49	0.0	7.16	<u>78.86</u>	75.41



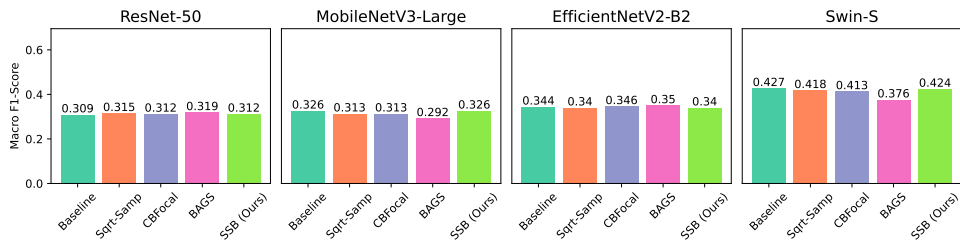
(a) WCS Camera Traps



(b) Snapshot Serengeti



(c) Caltech Camera Traps



(d) Wellington Camera Traps

**Fig. 4.** Comparison in terms of macro-averaged F1-score for all combinations of datasets and models. SSB achieved a score that was higher than the other long-tail visual recognition methods. It is worth mentioning that for the Swin-S model, the baseline obtained the best macro F1-score for all the datasets. SSB is the second best.



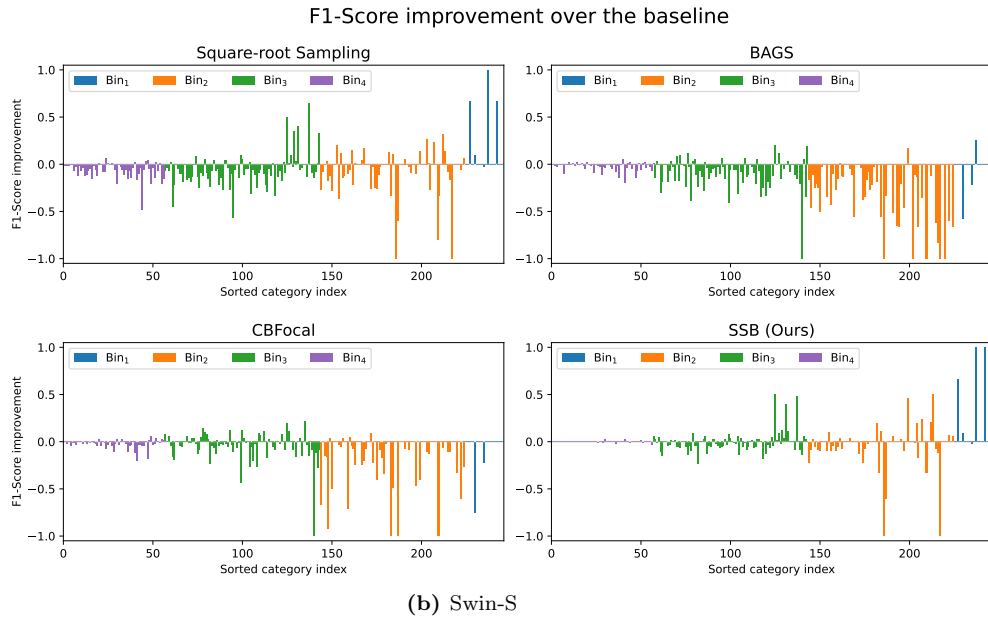
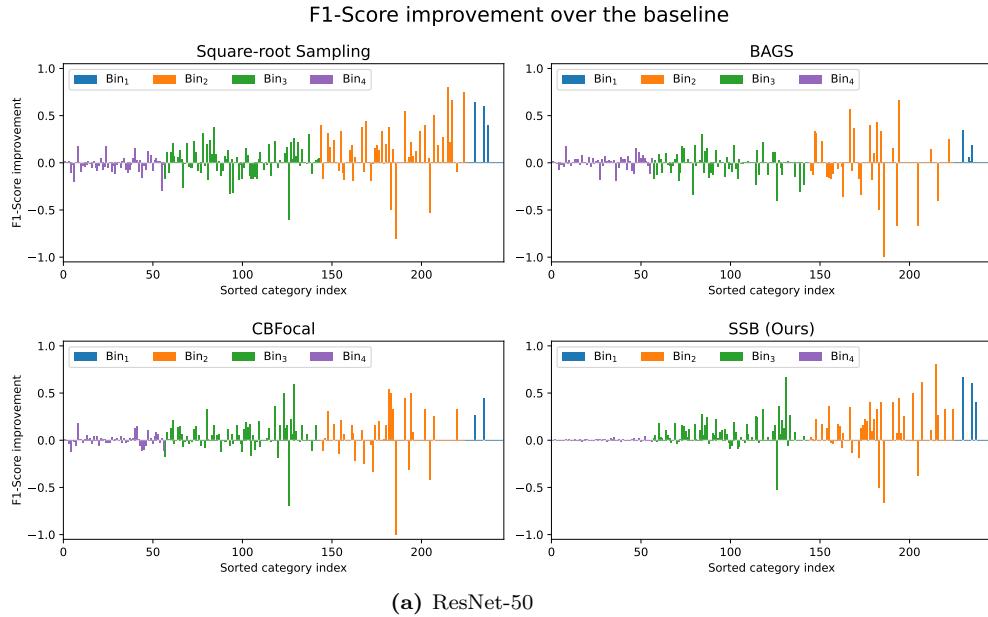


**Fig. 5.** Breakdown of F1-score improvement per class in the WCS dataset for the long-tail visual recognition methods over the baseline training procedure. For ResNet-50, our proposed SSB is the most consistent method to increase F1-score throughout the classes. Similar behavior occurs for MobileNetV3-Large and EfficientNetV2-B2 models (not included in the graph). However, for the Swin-S architecture, all the evaluated methods degraded the F1-score, but SSB is the one that lowers the F1-score the least.

**Table 5**

Results attained by different methods and models on different datasets when using the bounding box with the highest confidence as input. Bounding boxes were generated by MegaDetectorV4. Bold and underlined values, respectively, indicate the best and second-best result for each model and dataset combination.

Model	Training	WCS						Caltech CT				Wellington CT				
		$Acc_1$	$Acc_2$	$Acc_3$	$Acc_4$	$Acc_{all}$	$F_1^m$	$Acc_2$	$Acc_4$	$Acc_{all}$	$F_1^m$	$Acc_2$	$Acc_3$	$Acc_4$	$Acc_{all}$	$F_1^m$
ResNet-50	Baseline	0.00	21.68	52.94	90.61	87.85	0.429	0.00	60.59	56.87	0.423	0.0	8.18	<u>78.52</u>	75.14	0.408
	Sqrt-Samp	<u>20.00</u>	<b>43.47</b>	<b>67.19</b>	85.79	84.28	0.473	<b>0.24</b>	62.62	58.79	0.448	0.0	<u>22.21</u>	75.32	72.76	<b>0.431</b>
	CBFocal	3.75	26.33	61.67	<u>90.98</u>	<b>88.65</b>	0.468	0.00	64.32	60.37	0.458	0.0	10.77	78.47	75.21	<u>0.420</u>
	BAGS	<b>26.25</b>	23.16	53.33	<b>91.00</b>	<u>88.28</u>	0.414	<u>0.13</u>	<b>67.01</b>	<b>62.91</b>	<u>0.464</u>	0.0	<b>36.98</b>	77.92	<b>75.95</b>	0.409
	SSB (Ours)	17.50	<u>35.41</u>	<u>61.95</u>	90.39	88.25	<b>0.501</b>	0.11	<u>65.79</u>	<u>61.76</u>	<b>0.467</b>	0.0	12.23	<b>78.73</b>	<u>75.53</u>	0.416
MBNetV3	Baseline	0.00	26.11	55.93	<b>91.34</b>	<u>88.72</u>	0.434	0.00	64.80	60.82	<u>0.471</u>	0.0	11.89	<u>80.02</u>	76.74	0.434
	Sqrt-Samp	<b>26.25</b>	<b>42.22</b>	<b>64.41</b>	87.30	85.57	<u>0.458</u>	<u>0.29</u>	57.41	53.91	0.436	0.0	<u>23.89</u>	75.67	73.17	<b>0.441</b>
	CBFocal	1.25	19.64	56.86	91.04	88.39	0.418	0.13	61.29	57.53	0.468	0.0	11.44	79.30	76.03	0.422
	BAGS	13.75	22.47	45.07	90.13	87.07	0.373	<b>0.42</b>	<u>65.10</u>	<u>61.12</u>	0.461	0.0	<b>38.60</b>	79.31	<b>77.34</b>	0.403
	SSB (Ours)	<u>21.25</u>	<u>35.19</u>	<u>60.35</u>	<u>91.13</u>	<b>88.88</b>	<b>0.498</b>	0.11	<b>66.59</b>	<b>62.50</b>	<b>0.489</b>	0.0	15.98	<b>80.30</b>	<u>77.20</u>	<u>0.438</u>
EffV2-B2	Baseline	0.00	19.64	48.13	90.46	87.46	0.383	<u>0.11</u>	61.34	57.58	0.424	0.0	8.40	<u>79.61</u>	76.18	0.427
	Sqrt-Samp	<b>17.50</b>	<b>35.19</b>	<b>65.09</b>	88.37	86.49	<u>0.469</u>	0.08	60.33	56.63	0.437	0.0	<u>23.33</u>	76.86	74.28	<b>0.452</b>
	CBFocal	0.00	10.33	53.58	<b>91.34</b>	<b>88.40</b>	0.392	0.00	64.72	60.74	<u>0.468</u>	0.0	12.53	79.39	76.17	0.430
	BAGS	0.00	13.17	51.87	<u>91.24</u>	<u>88.26</u>	0.384	<b>0.61</b>	<b>68.03</b>	<b>63.89</b>	<b>0.478</b>	0.0	<b>44.22</b>	79.15	<b>77.46</b>	0.429
	SSB (Ours)	<u>16.25</u>	<u>30.31</u>	<u>60.28</u>	90.38	88.10	<b>0.474</b>	0.08	<u>67.10</u>	<u>62.98</u>	0.465	0.0	12.27	<b>79.80</b>	<u>76.55</u>	<u>0.439</u>
Swin-S	Baseline	16.25	53.35	78.20	<u>93.63</u>	<b>92.28</b>	<b>0.637</b>	<u>10.32</u>	<u>70.49</u>	<u>66.80</u>	<b>0.597</b>	0.0	11.25	<u>80.14</u>	<u>76.82</u>	0.503
	Sqrt-Samp	<b>25.00</b>	<b>62.09</b>	<b>79.37</b>	90.18	89.22	0.586	2.90	67.84	63.85	0.524	0.0	<b>19.05</b>	78.42	75.56	<u>0.504</u>
	CBFocal	8.75	39.95	75.24	<b>93.66</b>	<u>91.97</u>	<u>0.599</u>	<b>11.40</b>	69.41	65.84	<u>0.596</u>	0.0	9.41	79.25	75.88	0.476
	BAGS	8.75	33.83	69.93	93.52	91.52	0.511	8.29	<b>73.86</b>	<b>69.84</b>	0.560	0.0	<u>18.64</u>	79.36	76.44	0.447
	SSB (Ours)	<u>23.75</u>	<u>58.34</u>	<u>78.55</u>	93.53	<b>92.28</b>	<b>0.637</b>	3.27	69.52	65.45	0.576	0.0	12.34	<b>80.75</b>	<b>77.46</b>	<b>0.514</b>

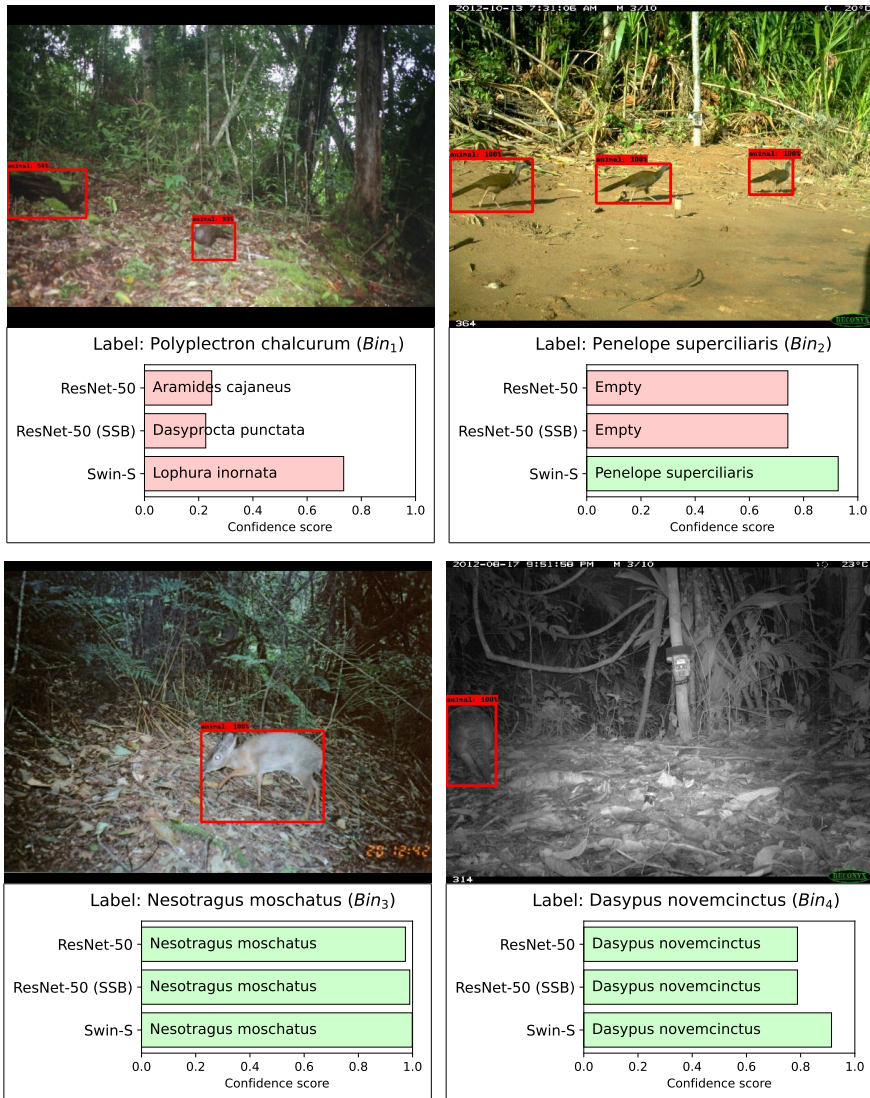


**Fig. 6.** Sample classification results for the baseline ResNet-50, ResNet-50 with the proposed SSB, and Swin-S. One picture was randomly picked from each bin of categories from the WCS dataset. Bounding boxes were generated using MegaDetectorV4.

### 3.3. Comparing SSB to one-stage training strategies

In this experiment, the performance of single-stage training methods was evaluated by applying re-weighting (CBFocal) and re-sampling (square-root sampling). For both methods, cropping was also used before classification, with bounding boxes being generated by MegaDetectorV4. Table 6 shows the results and compares them to the baseline training procedure and to our proposed two-stage SSB. The results show that square-root sampling presents similar behavior as observed in the two-stage training, i.e., improving the performance of the tail classes, but reducing the performance of the head classes. On the other hand, CBFocal obtained a great improvement over its results in two-stage training, and achieved the best overall accuracy in most cases. However, this improvement occurred mostly in the head classes. One-stage training methods also fail to improve the classification performance of the tail classes from the Caltech and Wellington datasets. Considering the objective of improving accuracy of the tail classes, our proposed SSB still represents the best trade-off between improving accuracy of the tail classes and reducing performance in the head classes.

**Table 6**

Comparing the results of one-stage training using square-root re-sampling and CBFocal loss with the baseline training procedure and our proposed SSB. Bold and underlined values, respectively, indicate the best and second-best result for each model and dataset combination.

Model	Training	WCS						Caltech CT				Wellington CT				
		$Acc_1$	$Acc_2$	$Acc_3$	$Acc_4$	$Acc_{all}$	$F_1^m$	$Acc_2$	$Acc_4$	$Acc_{all}$	$F_1^m$	$Acc_2$	$Acc_3$	$Acc_4$	$Acc_{all}$	$F_1^m$
ResNet-50	Baseline	0.00	21.68	52.94	<u>90.61</u>	87.85	0.429	0.00	60.59	56.87	0.423	0.0	8.18	78.52	75.14	0.408
	Sqrt-Samp	<b>20.00</b>	<b>45.86</b>	<b>71.61</b>	84.07	82.90	<u>0.530</u>	<b>0.90</b>	64.87	60.94	<u>0.529</u>	0.0	<u>13.58</u>	77.29	74.22	<u>0.458</u>
	CBFocal	15.00	<u>35.98</u>	<u>67.58</u>	<b>92.13</b>	<b>90.15</b>	<b>0.538</b>	0.05	<b>71.67</b>	<b>67.27</b>	<b>0.541</b>	0.0	<b>15.00</b>	<b>79.07</b>	<b>75.99</b>	<b>0.460</b>
	SSB (Ours)	<u>17.50</u>	35.41	61.95	90.39	<u>88.25</u>	0.501	<u>0.11</u>	65.79	61.76	0.467	0.0	12.23	<u>78.73</u>	<u>75.53</u>	0.416
MBNetV3	Baseline	0.00	26.11	55.93	<u>91.34</u>	88.72	0.434	0.00	<u>64.80</u>	<u>60.82</u>	0.471	0.0	11.89	80.02	76.74	0.434
	Sqrt-Samp	<b>22.50</b>	<b>48.13</b>	<b>71.75</b>	84.85	83.67	<b>0.504</b>	<b>1.08</b>	58.20	54.69	<u>0.487</u>	0.0	14.55	76.35	73.37	<b>0.459</b>
	CBFocal	3.75	24.86	<u>61.99</u>	<b>91.69</b>	<b>89.31</b>	0.463	0.08	64.23	60.29	0.485	0.0	<u>15.64</u>	<u>80.11</u>	<u>77.00</u>	<u>0.452</u>
	SSB (Ours)	<u>21.25</u>	<u>35.19</u>	60.35	91.13	<u>88.88</u>	<u>0.498</u>	<u>0.11</u>	<b>66.59</b>	<b>62.50</b>	<b>0.489</b>	0.0	<b>15.98</b>	<b>80.30</b>	<b>77.20</b>	0.438
EffV2-B2	Baseline	0.00	19.64	48.13	<u>90.46</u>	87.46	0.383	<u>0.11</u>	61.34	57.58	0.424	0.0	8.40	79.61	76.18	0.427
	Sqrt-Samp	<b>26.25</b>	<b>56.64</b>	<b>78.09</b>	85.66	84.84	<b>0.565</b>	<b>2.61</b>	61.37	57.76	<u>0.500</u>	0.0	<u>16.54</u>	77.07	74.15	<u>0.460</u>
	CBFocal	0.00	13.85	60.24	<b>92.37</b>	<b>89.72</b>	0.410	0.00	<b>71.39</b>	<b>67.00</b>	<b>0.529</b>	0.0	<b>18.60</b>	<b>80.75</b>	<b>77.76</b>	<b>0.471</b>
	SSB (Ours)	<u>16.25</u>	<u>30.31</u>	<u>60.28</u>	90.38	<u>88.10</u>	<u>0.474</u>	0.08	<u>67.10</u>	<u>62.98</u>	0.465	0.0	12.27	<u>79.80</u>	<u>76.55</u>	0.439
Swin-S	Baseline	16.25	53.35	78.20	<u>93.63</u>	<u>92.28</u>	<u>0.637</u>	<b>10.32</b>	<u>70.49</u>	<u>66.80</u>	<u>0.597</u>	0.0	11.25	80.14	76.82	0.503
	Sqrt-Samp	<b>23.75</b>	51.87	<b>78.62</b>	92.03	90.78	0.634	2.16	67.71	63.68	0.574	0.0	11.29	79.36	76.08	0.479
	CBFocal	<u>21.25</u>	<u>54.03</u>	78.41	<b>93.97</b>	<b>92.62</b>	<b>0.642</b>	<u>6.76</u>	<b>71.62</b>	<b>67.63</b>	<b>0.606</b>	0.0	<b>13.43</b>	<u>80.56</u>	<u>77.33</u>	<b>0.524</b>
	SSB (Ours)	<b>23.75</b>	<b>58.34</b>	<u>78.55</u>	93.53	<u>92.28</u>	<u>0.637</u>	3.27	69.52	65.45	0.576	0.0	<u>12.34</u>	<b>80.75</b>	<b>77.46</b>	<u>0.514</u>

#### 4. Discussion

The long-tail distribution is a characteristic of real-world tasks, such as visual recognition of species in camera-trap images, in which some classes concentrate the majority of available instances and a large number of classes have just a small quantity of samples. However, as indicated by Schneider et al. (2020), computer vision models generally often perform poorly on recognizing species in camera-trap images with fewer training instances (tail classes). In this work, a simple and effective framework called Square-root Sampling Branch (SSB) is proposed, which can improve the performance in tail classes with a minimal percentage of accuracy loss in the head classes. The proposed framework was systematically evaluated against state-of-the-art methods for handling the long-tail distribution issue in four different camera-trap datasets and four families of computer vision models. Our experiments show that our proposed framework presents competitive results with the methods in the literature, achieving the best trade-off between increasing the performance of the tail classes and reducing the head classes' accuracy in most cases.

Comparing our improved baseline training procedure with the literature, ResNet-50 achieved an overall accuracy of 92.79% for the Snapshot Serengeti dataset using the full image, while the same architecture achieved an accuracy of 93.6% in the work conducted by Norouzzadeh et al. (2018) and approximately 85% in that of Villa et al. (2017). However, while these works use burst or random split, in our methodology we split the training/test partitions based on locations, which tends to achieve a significantly lower accuracy, as demonstrated for other datasets by Beery et al. (2018), Schneider et al. (2020), and Tabak et al. (2019), in which the performance of models on untrained locations drops from 15% to 25% in accuracy in terms of absolute values. Furthermore, the categories and test sets used are different among the works, thus making the results not directly comparable. The same occurs when comparing our results for the Caltech CT dataset with the results from Beery et al. (2018). The lack of well-defined benchmarks for visual recognition of animal species in camera-

trap images makes it difficult to compare the results of different methods across works. Although most of the applications have their specificities and requirements regarding the data preparation or even the target dataset, it would be important to apply them using a standardized benchmark as well. However, designing such a benchmark dataset is challenging due to the wide variety of factors that need to be considered, including taxonomic coverage, biogeography, habitat and climate conditions, as well as the tasks to be included, such as species classification, long-tail visual recognition, animal detection, counting, and behavior identification. Therefore, it is recommended that the research community work collaboratively towards developing standardized benchmarks for automatic information extraction from camera-trap images, which would facilitate comparisons between different methods and ultimately lead to advancements in this field.

In general, the method that most improved the performance for the tail classes over the baseline was the square-root sampling. However, this method strongly degrades the head classes' accuracy. This behavior may be due to the high imbalance of the datasets, leading the square-root sampling to cause a high undersampling of the majority classes. Our proposed SSB can improve the accuracy for the tail classes more than CBFocal and BAGS for most of the cases, but, unlike square-root sampling, the degradation caused to the head classes is minimal, representing the best trade-off among all the evaluated methods. SSB also represents the best performance in terms of macro F1-score for most of the cases when compared with the two-stage methods. On the other hand, our experiments using one training stage show that CBFocal achieved the best overall accuracy for most of the cases, primarily because of its superior performance in the head classes. This CBFocal performance improvement may indicate that pretraining using softmax cross-entropy does not generate a good representation for fine-tuning using Focal loss, or that the learning of representation and classification is not well decoupled when using this loss function. However, our experiments were not designed to assess the performance based on representation (feature extractor) training strategies. Furthermore, Kang et al. (2020)

does not evaluate the performance of re-weighting methods when proposing the two-stage training approach. Although this approach was not explored in our experiments, a potential alternative could be to combine the outcomes of square-root resampling and CBFocal, which respectively performed better on the tail and head classes. However, this approach would require running inference using two models, effectively doubling the computational cost. In contrast, our proposed SSB only needs to be run once and is still competitive.

Looking into the model’s performance, Swin Transformer obtained the best results considering all the datasets, which was expected since this model has more parameters than the other selected models. It is worth noting that the Swin-S that was trained using the baseline settings attained an excellent performance even for the tail classes, reaching the best mean F1-score in most of the datasets. This superior performance of vision transformers in long-tail classification corroborates with what has been stated in the literature, as in the classification of fungi (Picek et al., 2022), for instance.

Regarding the question of whether using cropping before classification can improve model performance, when comparing the results of the first and the second series of experiments, it is possible to note a significant increase in the overall accuracy when applying cropping. This improvement is more relevant for the WCS and Caltech datasets, in which, for some cases, there was an improvement of 10% and 15%, respectively. This performance improvement is consistent with the results in the literature, for example, in (Beery et al., 2018), there was a 20% increase in the accuracy when cropping was used before classification. The use of an object detector as a preprocessing step before species identification is also part of the methodology of Schneider et al. (2018) and Norouzzadeh et al. (2021); however, its impact on the performance is not evaluated. Looking at the binned accuracy results, a performance increase is observed for all bins of the classes, except for the tail classes ( $Bin_2$ ) for the Caltech CT and Wellington CT datasets, in which all models and methods fail to learn them. The lowest performance increases due to the use of cropping before classification were observed for the Swin-S model, with an improvement

varying from 1% to 4%. It is worth noting that the accuracies for Swin-S using the full images are already very high when compared to the other models. This can be explained by the vision transformer’s attention mechanism that can allow it to focus on the animal even when using the full image.

Moreover, our experiments did not explain why the models were unable to learn to recognize the tail classes in the smaller datasets. The Caltech and Wellington datasets, with only 19 and 14 classes respectively, had a limited number of tail classes (4 and 1, respectively). It is possible that these tail classes were ignored due to the relatively low number of training samples available. To investigate this further, future studies could use the WCS dataset and progressively remove classes to evaluate the impact on model performance. This would also provide insights into the minimum number of training images per class needed to see an improvement in performance when using the evaluated methods.

One limitation to our study is that only the WCS dataset has classes belonging to all bins of classes in regards to the number of training instances. Another limitation is that, during our experiments, there was an effort to keep our settings as similar as possible across the methods and models in order to make a fair comparison; therefore, our hyperparameters are suboptimal and better tuning would lead to improvements.

## 5. Conclusions

Although rare or endangered species may be the classes of interest for projects using camera traps for monitoring wildlife, they are often neglected when developing deep-learning models for automatic species recognition, mostly because of the difficulty involved in learning classes with few training instances from long-tail datasets. In this work, a simple and effective framework called Square-root Sampling Branch (SSB) is proposed, which uses a multi-branch approach to improve the performance recognition of tail classes of long-tail camera-trap datasets with minimal loss in the performance recognition of the head classes.



Our proposed method was systematically evaluated against square-root sampling, CBFocal loss, and Balanced Group Softmax (BAGS) considering four camera-trap datasets: Snapshot Serengeti, WCS, Caltech CT, and Wellington CT. Our results showed that our proposed approach achieved the best trade-off between improving accuracy for the tail classes and decreasing the accuracy of the head classes, and is competitive with the state-of-the-art methods. It was also found that Swin-S performed better for most of the datasets even without applying any additional method for handling imbalance, and achieved an overall accuracy of 88.76% for the WCS dataset and 94.97% for the Snapshot Serengeti, when considering location-based splitting.

Despite the fact that our proposed framework improves the recognition of tail classes, our experiments clearly show that it is necessary to develop more sophisticated methods to handle the long-tail distribution in the recognition of species in camera-trap images. Specifically for the tail classes ( $Bin_1$  and  $Bin_2$ ), for which the results were extremely low, and especially for the small datasets, one could evaluate few-shot learning methods. Another issue that was discussed is the lack of standardized benchmarks for evaluating the performance of long-tail visual recognition of animal species when comparing new methods. It is hoped that our well-defined methodology for dataset preprocessing and training procedure helps establish good baselines for other researchers. In future works, other methods can be explored such as progressive-balanced sampling, Ally Complementary Experts, and Rebalanced Mixup (Remix). Additional training tricks, such as label smoothing and mixup, can also be performed, but they must be used with caution because one trick may affect the other.

### **Acknowledgements**

We would like to thank Coordenação de Aperfeiçoamento de Pessoal de Nível Superior– CAPES/PROAP. We also thank Fundação de Amparo à Pesquisa do Estado do Amazonas – FAPEAM/POSGRAD 2021. The present work is the result of the research and development (R&D) project No. 001/2020, between

the Federal University of Amazonas and FAEPI, Brazil, which has funding from Samsung, and uses resources from the Informatics Law for the Western Amazon (Federal Law nº 8.387/1991), and its disclosure is in accordance with article 39 of Decree No. 10.521/2020. The funders had no role in study design, data collection and analysis, decision to publish, or preparation of the manuscript.

## References

- Ahumada, J. A., Fegraus, E., Birch, T., Flores, N., Kays, R., O'Brien, T. G., Palmer, J., Schuttler, S., Zhao, J. Y., Jetz, W. et al. (2020). Wildlife insights: A platform to maximize the potential of camera trap and other passive sensor wildlife data for the planet. *Environmental Conservation*, 47, 1–6.
- Ahumada, J. A., Hurtado, J., & Lizcano, D. (2013). Monitoring the status and trends of tropical forest terrestrial vertebrate communities from camera trap data: a tool for conservation. *PloS one*, 8, e73707.
- Anton, V., Hartley, S., Geldenhuis, A., & Wittmer, H. U. (2018). Monitoring the mammalian fauna of urban areas using remote cameras and citizen science. *Journal of Urban Ecology*, 4. URL: <https://doi.org/10.1093/jue/juy002>. doi:10.1093/jue/juy002.
- Beery, S., Agarwal, A., Cole, E., & Birodkar, V. (2021). The iwildcam 2021 competition dataset. *arXiv preprint arXiv:2105.03494*, .
- Beery, S., Morris, D., Yang, S., Simon, M., Norouzzadeh, A., & Joshi, N. (2019). Efficient pipeline for automating species id in new camera trap projects. *Biodiversity Information Science and Standards*, 3, e37222.
- Beery, S., Van Horn, G., & Perona, P. (2018). Recognition in terra incognita. In *Proceedings of the European Conference on Computer Vision* (pp. 456–473).
- Bello, I., Fedus, W., Du, X., Cubuk, E. D., Srinivas, A., Lin, T.-Y., Shlens, J., & Zoph, B. (2021). Revisiting resnets: Improved training and scaling strategies. *Advances in Neural Information Processing Systems*, 34.

- Bengio, Y. (2012). Deep Learning of Representations for Unsupervised and Transfer Learning. In *Proceedings of ICML Workshop on Unsupervised and Transfer Learning* (pp. 17–36). JMLR Workshop and Conference Proceedings. URL: <https://proceedings.mlr.press/v27/bengio12a.html> iSSN: 1938-7228.
- Cai, J., Wang, Y., & Hwang, J.-N. (2021). Ace: Ally complementary experts for solving long-tailed recognition in one-shot. In *Proceedings of the IEEE/CVF International Conference on Computer Vision* (pp. 112–121).
- Chalmers, C., Fergus, P., Wich, S., & Montanez, A. C. (2019). Conservation ai: Live stream analysis for the detection of endangered species using convolutional neural networks and drone technology. *arXiv preprint arXiv:1910.07360*, .
- Chou, H.-P., Chang, S.-C., Pan, J.-Y., Wei, W., & Juan, D.-C. (2020). Remix: rebalanced mixup. In *European Conference on Computer Vision* (pp. 95–110). Springer.
- Cubuk, E. D., Zoph, B., Shlens, J., & Le, Q. V. (2020). Randaugment: Practical automated data augmentation with a reduced search space. In *Proceedings of the IEEE/CVF Conference on Computer Vision and Pattern Recognition Workshops* (pp. 702–703).
- Cui, Y., Jia, M., Lin, T.-Y., Song, Y., & Belongie, S. (2019). Class-balanced loss based on effective number of samples. In *Proceedings of the IEEE/CVF conference on computer vision and pattern recognition* (pp. 9268–9277).
- Cunha, F. (2021). iwildcam 2021 - ufam team. <https://github.com/alcunha/iwildcam2021ufam>.
- Cunha, F., dos Santos, E. M., Barreto, R., & Colonna, J. G. (2021). Filtering empty camera trap images in embedded systems. In *Proceedings of the IEEE/CVF Conference on Computer Vision and Pattern Recognition (CVPR) Workshops* (pp. 2438–2446).

- Elias, A. R., Golubovic, N., Krintz, C., & Wolski, R. (2017). Where’s the bear?-automating wildlife image processing using iot and edge cloud systems. In *2017 IEEE/ACM Second Inter. Conf. on Internet-of-Things Design and Implementation (IoTDI)* (pp. 247–258).
- Goodfellow, I., Bengio, Y., & Courville, A. (2016). *Deep learning*. MIT press.
- He, K., Zhang, X., Ren, S., & Sun, J. (2016a). Deep residual learning for image recognition. In *Proceedings of the IEEE conference on computer vision and pattern recognition* (pp. 770–778).
- He, T., Zhang, Z., Zhang, H., Zhang, Z., Xie, J., & Li, M. (2019). Bag of tricks for image classification with convolutional neural networks. In *Proceedings of the IEEE/CVF Conference on Computer Vision and Pattern Recognition* (pp. 558–567).
- He, Z., Kays, R., Zhang, Z., Ning, G., Huang, C., Han, T. X., Millsbaugh, J., Forrester, T., & McShea, W. (2016b). Visual informatics tools for supporting large-scale collaborative wildlife monitoring with citizen scientists. *IEEE Circuits and Systems Magazine*, *16*, 73–86.
- Howard, A., Sandler, M., Chu, G., Chen, L.-C., Chen, B., Tan, M., Wang, W., Zhu, Y., Pang, R., Vasudevan, V. et al. (2019). Searching for mobilenetv3. In *Proceedings of the IEEE/CVF International Conference on Computer Vision* (pp. 1314–1324).
- Kang, B., Xie, S., Rohrbach, M., Yan, Z., Gordo, A., Feng, J., & Kalantidis, Y. (2020). Decoupling representation and classifier for long-tailed recognition. In *International Conference on Learning Representations*.
- Kutugata, M., Baumgardt, J., Goolsby, J. A., & Racelis, A. E. (2021). Automatic camera-trap classification using wildlife-specific deep learning in nilgai management. *Journal of Fish and Wildlife Management*, *12*, 412–421.
- Li, Y., Wang, T., Kang, B., Tang, S., Wang, C., Li, J., & Feng, J. (2020). Overcoming classifier imbalance for long-tail object detection with balanced

- group softmax. In *Proceedings of the IEEE/CVF conference on computer vision and pattern recognition* (pp. 10991–11000).
- Lila.science (2022a). Caltech camera traps. <https://lila.science/datasets/caltech-camera-traps>. Accessed: 2022-04-01.
- Lila.science (2022b). Snapshot serengeti. <http://lila.science/datasets/snapshot-serengeti>. Accessed: 2022-03-17.
- Lila.science (2022c). Wcs camera traps. <https://lila.science/datasets/wcscameratraps>. Accessed: 2022-03-17.
- Lin, T.-Y., Goyal, P., Girshick, R., He, K., & Dollár, P. (2017). Focal loss for dense object detection. In *Proceedings of the IEEE international conference on computer vision* (pp. 2980–2988).
- Liu, Z., Lin, Y., Cao, Y., Hu, H., Wei, Y., Zhang, Z., Lin, S., & Guo, B. (2021). Swin transformer: Hierarchical vision transformer using shifted windows. In *Proceedings of the IEEE/CVF International Conference on Computer Vision* (pp. 10012–10022).
- Loshchilov, I., & Hutter, F. (2019). Decoupled weight decay regularization. In *International Conference on Learning Representations*.
- Norouzzadeh, M. S., Morris, D., Beery, S., Joshi, N., Jojic, N., & Clune, J. (2021). A deep active learning system for species identification and counting in camera trap images. *Methods in Ecology and Evolution*, 12, 150–161.
- Norouzzadeh, M. S., Nguyen, A., Kosmala, M., Swanson, A., Palmer, M. S., Packer, C., & Clune, J. (2018). Automatically identifying, counting, and describing wild animals in camera-trap images with deep learning. *Proceedings of the National Academy of Sciences*, 115, E5716–E5725.
- Picek, L., Šulc, M., Matas, J., Jeppesen, T. S., Heilmann-Clausen, J., Læssøe, T., & Frøslev, T. (2022). Danish fungi 2020-not just another image recognition

- dataset. In *Proceedings of the IEEE/CVF Winter Conference on Applications of Computer Vision* (pp. 1525–1535).
- Ren, S., He, K., Girshick, R., & Sun, J. (2015). Faster r-cnn: Towards real-time object detection with region proposal networks. In *Advances in neural information processing systems* (pp. 91–99).
- Russakovsky, O., Deng, J., Su, H., Krause, J., Satheesh, S., Ma, S., Huang, Z., Karpathy, A., Khosla, A., Bernstein, M., Berg, A. C., & Fei-Fei, L. (2015). ImageNet Large Scale Visual Recognition Challenge. *International Journal of Computer Vision (IJCV)*, *115*, 211–252. doi:10.1007/s11263-015-0816-y.
- Schindler, F., & Steinhage, V. (2021). Identification of animals and recognition of their actions in wildlife videos using deep learning techniques. *Ecological Informatics*, *61*, 101215.
- Schneider, S., Greenberg, S., Taylor, G. W., & Kremer, S. C. (2020). Three critical factors affecting automated image species recognition performance for camera traps. *Ecology and Evolution*, *10*, 3503–3517.
- Schneider, S., Taylor, G. W., & Kremer, S. (2018). Deep learning object detection methods for ecological camera trap data. In *2018 15th Conference on computer and robot vision (CRV)* (pp. 321–328). IEEE.
- Shashidhara, B. M., Mehta, D., Kale, Y., Morris, D., & Hazen, M. (2020). Sequence information channel concatenation for improving camera trap image burst classification. *arXiv preprint arXiv:2005.00116*, .
- Swanson, A., Kosmala, M., Lintott, C., Simpson, R., Smith, A., & Packer, C. (2015a). Data from: Snapshot serengeti, high-frequency annotated camera trap images of 40 mammalian species in an african savanna. URL: <https://doi.org/10.5061/dryad.5pt92>. doi:doi:10.5061/dryad.5pt92.
- Swanson, A., Kosmala, M., Lintott, C., Simpson, R., Smith, A., & Packer, C. (2015b). Snapshot serengeti, high-frequency annotated camera trap images of 40 mammalian species in an african savanna. *Scientific data*, *2*, 1–14.

- Tabak, M. A., Norouzzadeh, M. S., Wolfson, D. W., Newton, E. J., Boughton, R. K., Ivan, J. S., Odell, E. A., Newkirk, E. S., Conrey, R. Y., Stenglein, J. et al. (2020). Improving the accessibility and transferability of machine learning algorithms for identification of animals in camera trap images: Mlwic2. *Ecology and evolution*, *10*, 10374–10383.
- Tabak, M. A., Norouzzadeh, M. S., Wolfson, D. W., Sweeney, S. J., VerCauteren, K. C., Snow, N. P., Halseth, J. M., Di Salvo, P. A., Lewis, J. S., White, M. D. et al. (2019). Machine learning to classify animal species in camera trap images: Applications in ecology. *Meth. in Ecology and Evolution*, *10*, 585–590.
- Tan, M., & Le, Q. (2019). Efficientnet: Rethinking model scaling for convolutional neural networks. In *International conference on machine learning* (pp. 6105–6114). PMLR.
- Tan, M., & Le, Q. (2021). Efficientnetv2: Smaller models and faster training. In *International Conference on Machine Learning* (pp. 10096–10106). PMLR.
- Villa, A. G., Salazar, A., & Vargas, F. (2017). Towards automatic wild animal monitoring: Identification of animal species in camera-trap images using very deep convolutional neural networks. *Ecological informatics*, *41*, 24–32.
- Wang, X., Lian, L., Miao, Z., Liu, Z., & Yu, S. (2021). Long-tailed recognition by routing diverse distribution-aware experts. In *International Conference on Learning Representations*.
- Wightman, R., Touvron, H., & Jégou, H. (2021). Resnet strikes back: An improved training procedure in timm. *arXiv preprint arXiv:2110.00476*, .
- Willi, M., Pitman, R. T., Cardoso, A. W., Locke, C., Swanson, A., Boyer, A., Veldthuis, M., & Fortson, L. (2019). Identifying animal species in camera trap images using deep learning and citizen science. *Methods in Ecology and Evolution*, *10*, 80–91.

- Xi, T., Wang, J., Qiao, H., Lin, C., & Ji, L. (2021). Image filtering and labelling assistant (ifla): Expediting the analysis of data obtained from camera traps. *Ecological Informatics*, *64*, 101355.
- Yang, D.-Q., Li, T., Liu, M.-T., Li, X.-W., & Chen, B.-H. (2021a). A systematic study of the class imbalance problem: Automatically identifying empty camera trap images using convolutional neural networks. *Ecological Informatics*, *64*, 101350.
- Yang, D.-Q., Ren, G.-P., Tan, K., Huang, Z.-P., Li, D.-P., Li, X.-W., Wang, J.-M., Chen, B.-H., & Xiao, W. (2021b). An adaptive automatic approach to filtering empty images from camera traps using a deep learning model. *Wildlife Society Bulletin*, *45*, 230–236.
- Yang, D.-Q., Tan, K., Huang, Z.-P., Li, X.-W., Chen, B.-H., Ren, G.-P., & Xiao, W. (2021c). An automatic method for removing empty camera trap images using ensemble learning. *Ecology and Evolution*, *11*, 7591–7601.
- Yousif, H., Yuan, J., Kays, R., & He, Z. (2019). Animal scanner: Software for classifying humans, animals, and empty frames in camera trap images. *Ecology and evolution*, *9*, 1578–1589.
- Zhang, X., Zhou, X., Lin, M., & Sun, J. (2018). Shufflenet: An extremely efficient convolutional neural network for mobile devices. In *Proceedings of the IEEE conference on computer vision and pattern recognition* (pp. 6848–6856).
- Zhang, Y., Wei, X.-S., Zhou, B., & Wu, J. (2021). Bag of tricks for long-tailed visual recognition with deep convolutional neural networks. In *Proceedings of the AAAI Conference on Artificial Intelligence* (pp. 3447–3455). volume 35.
- Zhou, B., Cui, Q., Wei, X.-S., & Chen, Z.-M. (2020). Bbn: Bilateral-branch network with cumulative learning for long-tailed visual recognition. In *Proceedings of the IEEE/CVF conference on computer vision and pattern recognition* (pp. 9719–9728).



Zhu, H., Tian, Y., & Zhang, J. (2022). Class incremental learning for wildlife biodiversity monitoring in camera trap images. *Ecological Informatics*, (p. 101760).

Zualkernan, I., Dhou, S., Judas, J., Sajun, A. R., Gomez, B. R., & Hussain, L. A. (2022). An iot system using deep learning to classify camera trap images on the edge. *Computers*, *11*, 13.

Zualkernan, I. A., Dhou, S., Judas, J., Sajun, A. R., Gomez, B. R., Hussain, L. A., & Sakhmini, D. (2020). Towards an iot-based deep learning architecture for camera trap image classification. In *2020 IEEE Global Conference on Artificial Intelligence and Internet of Things (GCAIoT)* (pp. 1–6). IEEE.